Materials Research. 2015; 18(3): 608-613
DOI: http://dx.doi.org/10.1590/1516-1439.019015

Comparison of Kinetic Study of CTMA$^+$ Removal of Molecular Sieve Ti-MCM-41 Synthesized with Natural and Commercial Silica

***Maria do Socorro Braga Fontes*[a]*, *Dulce Maria de Araújo Melo*[b], *Cintia de Castro Costa*[c], *Renata Martins Braga*[d], *Marcus Antonio de Freitas Melo*[e], *José Antônio Barros Leal Reis Alves*[f]**

[a]*Programa de Pós-Graduação em Ciência e Engenharia de Materiais – PPGCEM, Universidade Federal do Rio Grande do Norte – UFRN, Campus Universitário Lagoa, Natal, RN, Brazil*
[b]*Departamento de Química, Universidade Federal do Rio Grande do Norte – UFRN, Natal, RN, Brazil*
[c]*Programa de Pós-Graduação em Ciência e Engenharia de Petróleo – PPGCEP, Universidade Federal do Rio Grande do Norte – UFRN, Natal, RN, Brazil*
[d]*Escola Agrícola de Jundiaí – EAJ, Universidade Federal do Rio Grande do Norte – UFRN, Macaíba, RN, Brazil*
[e]*Departamento de Engenharia Química, Universidade Federal do Rio Grande do Norte – UFRN, Natal, RN, Brazil*
[f]*Departamento de Química, Universidade Federal do Rio Grande do Norte – UFRN, Natal, RN, Brazil*

Received: April 1, 2015; Revised: April 28, 2015

This work aimed to determine and compare the apparent activation energy, involved in thermal decomposition of CTMA$^+$ from the pores of Ti-MCM-41 synthesized by two different source of silica in order to evaluate their influence in the template removal. The molecular sieves Ti-MCM-41 were synthesized using rice husk ash (RHA), as alternative low cost source of silica, and commercial silica gel, obtaining two mesoporous material by hydrothermal synthesis of gel molar composition of: 1.0 CTMABr: 4.0 SiO_2: X TiO_2: 1.0 Na_2O: 200.0 H_2O. The samples were characterized to compare its properties by X-ray diffraction, IR spectroscopy, BET method and thermogravimetric analysis (TGA). The kinetic study using the model proposed by Flynn and Wall to determine the apparent activation energy for CTMA$^+$ removal was performed using TGA data. The thermogravimetric analysis results of the material obtained from RHA confirmed intrinsic properties of mesoporous MCM-41 as the synthesized with commercial silica gel, such as high specific area, mesoporous range of pore diameter and hexagonal structure. According to the kinetics results the RHA showed similar chemical interaction to commercial silica gel, which makes it an interesting material, since it is a low cost source of natural silica from agricultural waste.

Keywords: *Ti-MCM-4, rice husk ash, molecular sieve, kinetic*

1. Introduction

During the recent years, intensive research activity has been focused on mesoporous materials like MCM-41[1-6]. The MCM-41 shows no considerable acidity, limiting their direct use in catalytic reactions. However, due to its high specific area, they are excellent catalyst supports, which can generate acid/base sites during or after synthesis either by impregnation or by isomorphous substitution of heteroatom in the MCM-41, especially metals incorporation such as Al, Ti, Zr, B, V, etc[7]. The introduction of titanium in MCM-41 was reported for the first time in 1994[8]. The iso and nonisomorphic substitutions usually enhance catalytic activity in processes of commercial interest such as: hydrocarbon catalytic cracking isomerization, hydrodesulphurization, oxidation reactions, hydroxylation and epoxidation of aromatics, olefins and phenols[9].

Many authors[10-12] have used the rice husk ash (RHA) as silica source in the synthesis of various mesoporous materials (ZSM-5, MCM-41, MCM-48, SBA-15) using different extraction methods of silica. This agricultural waste has attracted great interest from researchers due to its high silicon content (>90%) of low cost that can be use as Si source in different silica based materials.

The synthesis of Ti-MCM-41 takes place by mixing the silica source and template, which is usually a long-chain surfactant that give micelles, which originate tubes forming hexagonally ordered structure characteristic of MCM-41. The gel prepared with these reagents at different molar ratios surfactant/silicon is subjected to a hydrothermal treatment in alkaline conditions, then washed and dried at room temperature. The template removal, which occur by calcination at approximately 550 °C, results in a silicon material of high specific area and large diameters porous. The synthesis conditions can be changed with the purpose of obtaining materials with different properties. The factors affecting the final product are molar ratio template/silica

---

*e-mail: socorro.fontes@yahoo.com.br

concentration and length of the carbon chain of the template, synthesis temperature, pH and nature of silica[13].

This work aims the use of the rice husk ash (RHA) and commercial silica gel (SG) as alternatives source of silica in the synthesis of Ti-MCM-41, performing the kinetic study of surfactant cetyltrimethyl ammonium bromide ($CTMA^+$) removal, using the model proposed by Flynn-Wall, trough thermogravimetric analysis data, relating the apparent activation energy with the chemical interaction of silica sources and the template $CTMA^+$ used in synthesis of this material.

2. Experimental Procedure

2.1. Silica extraction

The rice husk (RH) collected at Rio Grande do Norte State, northeast of Brazil was washed in hot water 60 °C, under constant stirring for 1 h, dried at 100 °C for 12 h. After it was crushed in a knife mill (TECNAL TE 631), sieved at 150 mesh (0.106 mm) and calcined in a muffle furnace (TECNAL 3000) at 600 °C, de 10 °C min^{-1} for 2 h. The resultant material (RHA) was used as silica source in the synthesis of Ti-MCM-41.

2.2. Hydrothermal synthesis

The synthesis of the molecular sieve MCM-41 was conducted hydrothermally from molar ratio of 1.0 CTMABr: 4.0 SiO_2: X TiO_2: 1.0 Na_2O: 200.0 H_2O. The "X" value was set to the molar ratio Si/Ti equal to 50. The silica dispersion and CTMABr solution was submitted to stirring for 1 h and transferred to a stainless steel autoclave heated in an oven at 100 °C for 5 days. The pH correction were made daily in the range 9–10 with a 30% acetic acid solution until it reach stability. The material was filtered and washed with a 2% solution of HCl in ethanol and then with distilled water. The material resulting from the crystallization process was dried at 100 °C for 4 h. Finally, the solid resulting was subjected to TGA analysis for analyze the better calcination condition according kinetic study.

2.3. Characterization

X-ray diffraction (XRD) analyses were conducted on equipment Shimadzu XRD-7000 using a Cu-Kα radiation source with voltage of 30kV, current of 30 mA and Ni filter. Data were collected in the 2θ range from 1 to 10°. FTIR analyses were performed using Shimadzu Fourier transform infrared spectrophotometer model IR - Prestige 21 using KBr disks. For the KBr disks preparation, the samples were dried in an oven at 100 °C for 2 hours, and then mixed (2 w/w% concentration) with solid KBr, the material obtained was hydraulically pressed (Carver Press) with five tons and the disks were submitted to analysis, whose spectra were scanned in the region from 4000 to 400 cm^{-1}. The specific area of the samples was determined by nitrogen adsorption at 77 K using the BET method in a Quantachrome NOVA 2000 instrument. Before the nitrogen measurement, samples were degassed at 300 °C in helium for 3 h. The wall thickness (w) of MCM-41 was obtained by the difference between the lattice parameter a_0 and the pore diameter (dp). The thermogravimetric analysis were performed in a thermobalance, model TGA-60 Shimadzu using a nitrogen atmosphere, with a flow rate of 50 $ml.min^{-1}$ in the temperature range of 30 to 600 °C, the heating rate of 5, 10 and 20 °C min^{-1}.The UV-Vis analysis were performed in infrared spectrophotometer model Shimadzu, UV-2450.

2.4. Kinetic methods

The kinetic study consists in determining the decomposed fraction (α) as a function of reaction time (t) for processes in which the temperature is kept constant or in processes in which the temperature varies linearly with time. In thermogravimetric analysis (TGA), the fraction decomposed (α) is defined by Equation 1. The decomposition rate of $CTMA^+$ from the pores of Ti-MCM-41 depends on temperature (**T**), conversion (α) and reaction time (**t**). In the TGA, the conversion of CTMA+ is expressed by (Equation 1).

$$\alpha = \frac{\left(m_o - m_t\right)}{\left(m_o - m_f\right)} \tag{1}$$

Where: $\boldsymbol{m_o}$ is the initial mass, $\boldsymbol{m_f}$ is the final mass, and $\boldsymbol{m_t}$ is the Ti-MCM-41 mass, which varies with time.

The decomposition rate of $CTMA^+$ can be expressed by Equation 2, where the reaction rate is related to the sample decomposition.

$$\frac{d\alpha}{dt} = K\left(1-\alpha\right)^{n} \tag{2}$$

Where K is a constant rate obtained by Arrhenius equation, (Equation 3).

$$K = Ae^{-E/RT} \tag{3}$$

The determination of global kinetic parameters via TGA was based on method proposed by Flynn–Wall that involves measuring the temperature corresponding to fixed values of conversion (α) from experiments at different heating rates (β), and plotting log (β) against 1/T giving straights lines with slopes -Ea/R[14]. This model require at least three dynamic curves with different and constant heating rates (β); in this work it was assumed as 5, 10, and 20 °C min^{-1} with temperature between 30 and 900 °C, mass of the samples was approximately 3 mg. This model was used to determine the apparent activation energy (Equation 4) and conversion (α) as a function of temperature.

$$\mathrm{Ea} = -\left(\frac{\mathrm{R}}{\mathrm{b}}\right)\times\left(\partial\ \log\beta\right)/\,(\partial\left(\frac{1}{\mathrm{T}}\right) \tag{4}$$

Where β is the heating rate, **T** is the absolute temperature (K), **b** is an interaction variable, **R** is the universal gas constant and **Ea** is the activation energy (J mol^{-1}).

3. Results and Discussion

The thermogravimetric curves of Ti-MCM-41 (SG) and Ti-MCM-41 (RHA) in different heating ratios are shown in Figure 1a, b, respectively. The mass loss is related to the following stages: (1) desorption of water physically adsorbed in the pores of the material from 30 – 100 °C, (2) decomposition of the surfactant CTMABr between 145 and 280 °C, (3) third event occurs at temperatures above

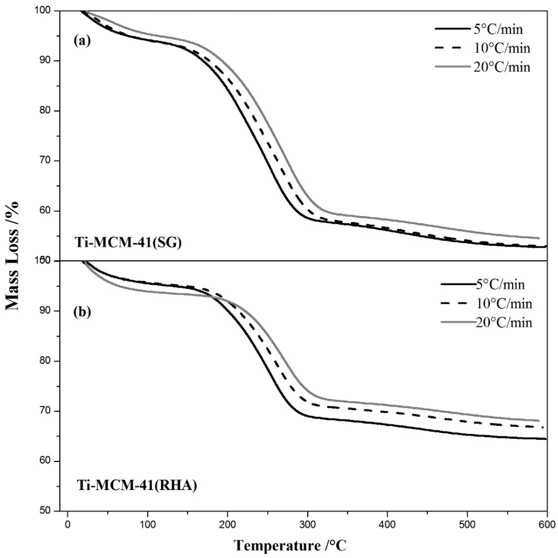

Figure 1. TG curves of (a) Ti-MCM-41 (SG) and (b) Ti-MCM-41 (RHA).

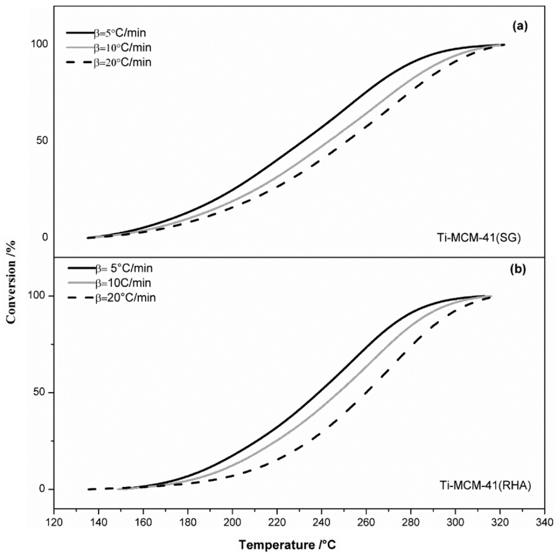

Figure 2. Conversion curve versus temperature of the Ti-MCM-41 (a) (SG) and (b) (RHA) (with heating rates of 5, 10, 20 °C / min $^{-1}$).

335 °C due to water loss by condensation of silanol groups of the inner surface of pores, which interacted with the molecular sieve. The analysis of samples was performed in order to obtain the best calcinations conditions for CTMA$^+$ removal as well as the temperature range where these molecules are removed. These data are fundamental to determine the lowest calcination temperature required for the CTMA$^+$ removal from the pores of material[15].

The kinetic study was carried out in the temperature range of CTMA$^+$ removal from 140 to 335°C. The Figure 2 show the conversion curve versus temperature of the Ti-MCM-41 (a) (SG) and (b) (RHA). It can be seen that for a given temperature there are different percentages of conversion for the different heating rates (β = 5, 10 and 20 °C min^{-1}). The logarithm of the heating rates (log (β)) was plotted versus the inverse of the conversion temperature ($1/T_{\alpha}$) for the three curves (β), straight lines were obtained (Figure 3) in which the slope of each line corresponds to -Ea/R, where R is the gas constant[16]. The linearity confirms that the kinetic model adopted can be used to evaluate the degradation of CTMA$^+$ through thermogravimetry analysis.

According to results of Table 1, that show the values of apparent activation energy for conversion levels from 5 to 90 %, the presence of titanium in the MCM-41 favor minor apparent activation energy values for CTMA$^+$ removal from the porous system of Ti-MCM-41 (SG) and (RHA) compared to RHA-MCM-41 and MCM-41 synthesized by Braga *et al.* [10] and Souza et al.[15], that found values of Ea of 221 and 166 kJ mol^{-1}, respectively[15,17]. In previous study Fontes et al.[1] observed that the increase of Ti in MCM-41 resulted in a gradual decrease apparent activation energy for CTMA$^+$ removal, which confirm the lower Ea values to the Ti-MCM-41 (SG) and (RHA) when compared to other MCM-41 of literature[18]. According to Braga et al.[17] the hydrophilic part of surfactant, which has positive charge, interacts with the surface of the pore of mesoporous MCM-41 material via coulomb forces. The apparent activation energy

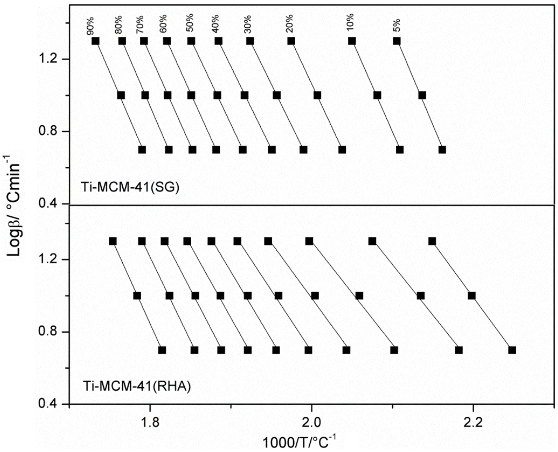

Figure 3. Logarithmic of the heating rate as a function of the inverse of temperature of the Ti-MCM-41 (a) (SG) and (b) (RHA) (β of 5, 10, 20 °C min $^{-1}$).

Table 1. Apparent activation energy for the conversion values (α) from 5 to 90%.

Conversion /%	Ti-MCM-41(SG) Ea / KJmol^{-1}	Ti-MCM-41(RHA) Ea / KJmol^{-1}
5	145.40	110.67
10	138.51	101.90
20	130.42	103.23
30	124.51	111.53
40	124.49	123.47
50	128.90	136.25
60	135.27	145.67
70	136.94	156.15
80	142.29	168.45
90	141.91	179.61
Average	**134.7**	**133.6**

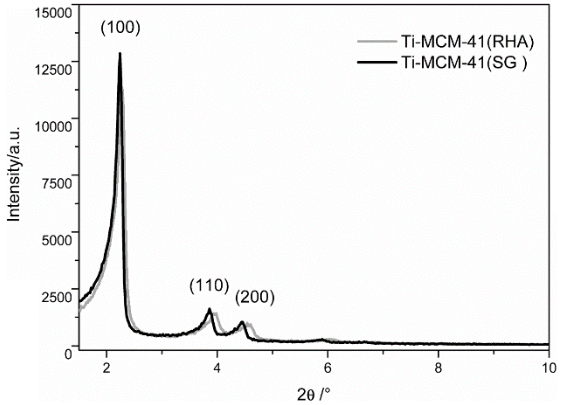

Figure 4. XRD patterns of Ti-MCM -41(SG) and Ti-MCM-41 (RHA).

involved in the removal of CTMA$^+$ located within the pores of molecular sieve provides the magnitude of the interactions between the template and silica[17]. The Ti-MCM-41 (SG) and Ti-MCM-41 (RHA) showed near values for the two silica sources used confirming that the RHA showed similar chemical interaction as commercial silica used in the synthesis of Ti-MCM-41. These results suggest that there was a possible interaction of Ti contained in the MCM-41 structure with CTMA$^+$ species used in the MCM-41 synthesis, facilitating the director removal.

For the XRD result, shown in Figure 4, the Ti-MCM-41 (SG) and Ti-MCM-41 (RHA) clearly exhibited patterns XRD (100), (110) and (200) that are reflections planes typical of hexagonal structures. The XRD patterns of the synthesized samples are similar to MCM-41 materials reported in literature[1,10,19]. Both samples showed high intensity of peaks.

In the infrared absorption spectra (Figure 5) of the Ti-MCM-41 (SG) (a) and Ti-MCM-41 (RHA) (b) was observed the presence of a broad band around 3250 and 3720 cm^{-1} referent to hydroxyl groups of internal and external mesoporous structure[20]. The band around 960 cm^{-1} could be attributed to Si-O-Ti vibrations formed, to which is attributed the large amount of silanol groups present[21-22]. When titanium is incorporated into the MCM-41 molecular sieve, there was an increase in intensity of this band. According to Gomes[21] this band is due to the large number of silanol groups in its structure, becoming more intense when metals are incorporated into MCM-41 structure. However, this information needs more effort analytical and will be confirmed through UV-Vis.

The UV-vis spectra of Ti-MCM-41 (SG) and Ti-MCM-41 (RHA), shown in Figure 6, indicate that the materials contain mainly isolated Ti species incorporated in the silicate structure, as they present well defined band at ~ 210 nm. The 254 nm band is due to the presence of Ti atom bonded to four silica tetrahedral. This band was assigned to the charge transfer from the Si, Ti-linking oxygen atoms to the Ti (IV) central atom in directions perpendicular to the Ti–O–Ti chains. The inexistence of the absorption band 370 nm indicate the absence of anatase TiO_2 in the final products.[23,24]

The XRF analysis was used to determine the chemical composition of mesoporous material after calcination, and according to result shown in Table 2 it was possible to

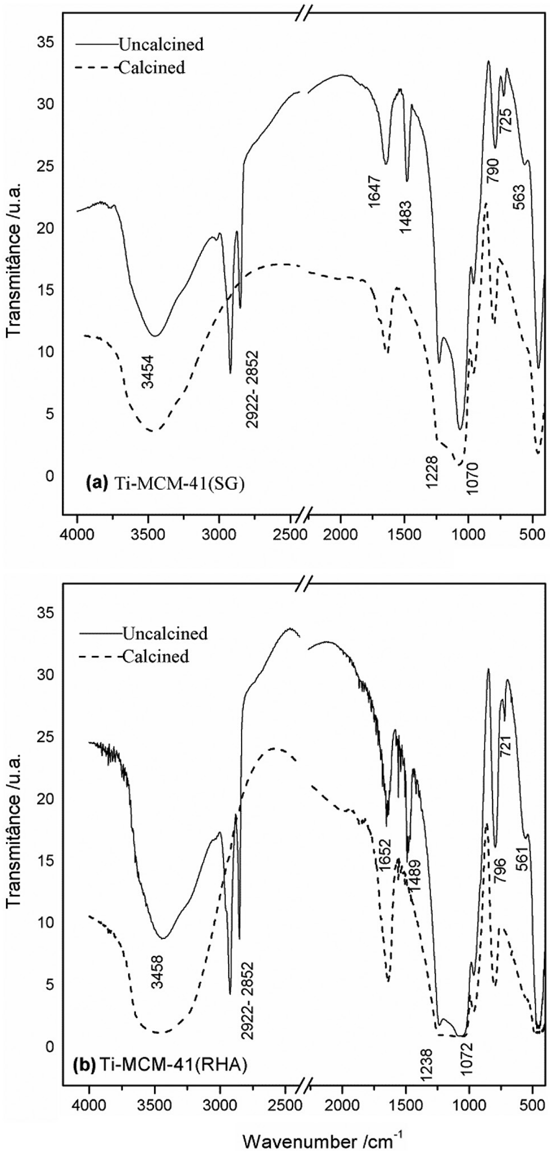

Figure 5. FTIR spectra of calcined and uncalcined of TiMCM-41(SG) and Ti-MCM-41 (RHA).

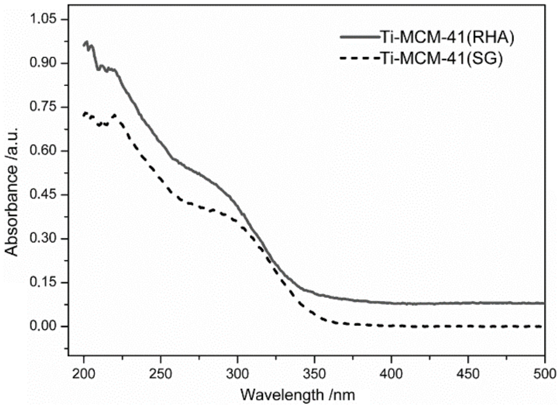

Figure 6. UV-vis of Ti-MCM -41(SG) and Ti-MCM-41 (RHA) samples.

Table 2. Chemical composition of Ti-MCM-41 (SG) and Ti-MCM-41 (RHA).

Samples	Si (%/wt)	Ti(%/wt)	Others
Ti-MCM-41(SG)	91.2	3.3	5.5
Ti-MCM-41(RHA)	90.3	3.9	5.8

Table 3. Adsorption parameters for theTi-MCM-41 (SG) and Ti-MCM-41(RHA).

Samples	S_{BET}/m^2g^{-1}	d_p a/nm	$V_p cm^3g^{-1}$	a_o b/nm	W= a_o–d_p/nm
Ti-MCM-41(SG)	678	3.27	0.59	4.86	1.59
Ti-MCM-41(RHA)	676	3.54	0.59	4.55	1.0

[a]Calculated from the desorption branch by BJH method. [b]Cell parameter (calculated from $a_0 = 2d_{100}/$ (nm).

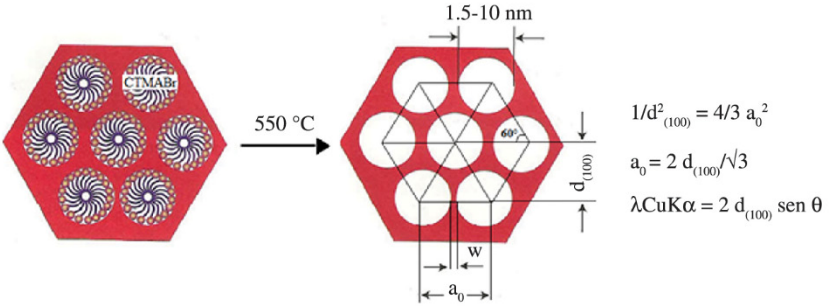

Figure 7. Representation of MCM-41 before and after calcination. Where: w – wall thickness of silica, $\mathbf{a_0}$-lattice parameter and d(100) - interplanar distance to plane 100. Figure from Braga et al.[10].

confirm the presence of Ti in both materials Ti-MCM-41 (SG) and Ti-MCM-41 (RHA), respectively.

The textural parameters for the Ti-MCM-41 (SG) and Ti-MCM-41(RHA) are show in Table 3. The wall thickness of the silica that forms the hexagonal structure of Ti-MCM-41 was obtained by the difference in lattice parameter a_0 (XRD) (Figure 7) and pore diameter dp (BET), where it is observe a high specific surface area and the similarity between the pore size of the two materials, and they are in accordance with the materials synthesized by Mobil researchers Oil Research and Development Co.[19]. These results highlight the importance of choosing appropriately source of silica to synthesize MCM-41. Table 3 shows that the presence of titanium in the MCM-41 structure caused an increase in the pore diameter and consequently a slight reduction in the wall thickness when compared to pure MCM-41[10] (dp = 3.2; S_{BET} = 897 m^2g^{-1}), confirming the presence of metal cation in the network. According to literature, increasing titanium content in the synthesis mixture results in an increase in the lattice parameter (a_0) and this change is probably due to the greater length of the Ti–O bond (1.80 Å) when compared to the Si-O bond (1.61 Å)[21]. According to Eimer et al.[23] when the Ti content increases the surface area of MCM-41 decreases which is clearly correlated to the decrease in the structural order observed, the same result was observed by Fontes et al.[18,23]. This result could be attributed to the differences in the ionic radio of Ti^{4+} (0.68 Å) and Si^{4+} (0.41 Å), the substitution of the larger Ti^{4+} ion in place of Si^{4+} invariably should distort the geometry around Ti from an ideal Td. Therefore, the length of Ti–O–Si bond, different from that of Si–O–Si, should lead to structure deformation[24].

4. Conclusion

Based on the characterization results, the catalyst Ti-MCM-41 was successfully synthesized using RHA and SG as silica source, it can be concluded that RHA is a suitable source of silica for synthesis, since the material obtained showed intrinsic properties of a mesoporous material MCM-41. The RHA besides be a low cost source of natural silica is derived from a residue generated in rice production. Thus, the use of RHA in the synthesis of Ti-MCM-41 adds value to the residue and reduces the environmental impacts caused by its disposal.

According to the model of Flynn Wall the apparent activation energy (Ea) for the decomposition of surfactant $CTMA^+$ occluded in the pores of Ti-MCM-41 (SG) and Ti-MCM-41 (RHA) showed near values for the two silica sources used, confirming that the RHA showed similar chemical interaction as commercial silica gel used in the synthesis of Ti-MCM-41.

Acknowledgements

The authors gratefully acknowledge the Refine and Catalyses Laboratories (NUPRAR/LCR) at UFRN, the Post-Graduation Program in Science and Engineering of Petroleum and Materials (PPGCEP/PPGCEM) and CAPES (Improve Coordination of Superior Academic Level People) for the financial support and scholarship provided.

References

1. Fontes MSB, Melo DMA, Barros JMF, Braga RM and Rodrigues V. Kinetic study of CTMA+ removal from the pores of the Ti-MCM-41 molecular sieve. *Materials Research*. 2014; 17(Suppl 1):216-221. http://dx.doi.org/10.1590/1516-1439.217113.
2. Meynen V, Cool P and Vansant EF. Verified syntheses of mesoporous materials. *Microporous and Mesoporous Materials*. 2009; 125(3):170-223. http://dx.doi.org/10.1016/j.micromeso.2009.03.046.
3. Pal N and Bhaumik A. Soft templating strategies for the synthesis of mesoporous materials: inorganic, organic-inorganic hybrid and purely organic solids. *Advances in Colloid and Interface Science*. 2013; 21:189-190. PMid:23337774.
4. Belmabkhout Y, Serna-Guerrero R and Sayari A. Adsorption of CO2-containing gas mixtures over amine-bearing pore-expanded MCM-41 silica: application for CO2 separation. *Adsorption*. 2011; 17(2):395-401. http://dx.doi.org/10.1007/s10450-011-9348-0.
5. Kamarudin KSN and Alias N. Adsorption performance of MCM-41 impregnated with amine for CO2 removal. *Fuel Processing Technology*. 2013; 106:332-337. http://dx.doi.org/10.1016/j.fuproc.2012.08.017.
6. Costa CC, Melo DMA, Melo MAF, Mendoza ME, Nascimento JC, Andrade JM, et al. Effects of different structure-directing agents (SDA) in MCM-41 on the adsorption of CO2. *Journal of Porous Materials*. 2014; 21(6):1069-1077. http://dx.doi.org/10.1007/s10934-014-9857-9.
7. Klimova-Berestneva T, Martínez-Rosales JM, Ramírez-Solís J. Effect of surfactant removal method on the texture of Ti(R) MCM-41. *Revista Mexicana de Ingeniería Química*. 2002; 1:105–110
8. Galacho C, Ribeiro Carrott MML and Carrott PJM. Structural and catalytic properties of Ti-MCM-41 synthesised at room temperature up to high Ti content. *Microporous and Mesoporous Materials*. 2007; 100(1-3):312-321. http://dx.doi.org/10.1016/j.micromeso.2006.11.018.
9. Araújo RS, Azevedo DCS, Rodríguez-Castellón E, Jiménez-López A and Cavalcante CL Jr. Al and Ti-containing mesoporous molecular sieves: synthesis, characterization and redox activity in the anthracene oxidation. *Journal of Molecular Catalysis A Chemical*. 2008; 281(1-2):154-163. http://dx.doi.org/10.1016/j.molcata.2007.09.001.
10. Braga RM, Teodoro NM, Melo DMDA, Aquino FM, Barros JMF and Freitas JCO. Síntese da peneira molecular MCM-41 derivada da cinza da casca do arroz. *Holos*. 2013; 5:40-49. http://dx.doi.org/10.15628/holos.2013.1364.
11. Chareonpanich M, Namto T, Kongkachuichay P and Limtrakul J. Synthesis of ZSM-5 Zeolite from Lignite Fly Ash and Rice Husk Ash. *Fuel Processing Technology*. 2004; 85(15):1623-1634. http://dx.doi.org/10.1016/j.fuproc.2003.10.026.
12. Bajpai PK, Rao MS and Gokhale KVGK. Synthesis of mordenite type zeolite using silica from rice husk ash. *Industrial & Engineering Chemistry Product Research and Development*. 1981; 20(4):721-726. http://dx.doi.org/10.1021/i300004a026.
13. Schüth F. Surface properties and catalytic performance of novel mesostructured oxides. *Berichte der Bunsengesellschaft fur Physikalische Chemie*. 1995; 99(11):1306-1315. http://dx.doi.org/10.1002/bbpc.199500076.
14. Flynn JH and Wall LA. A quick, direct method for the determination of activation energy from thermogravimetry data. *Journal of Polymer Science Part B: Polymer Letters*. 1966; 4(5):323-328. http://dx.doi.org/10.1002/pol.1966.110040504.
15. Souza MJB, Silva AOS, Aquino JMFB, Fernandes VJ Jr and Araújo AS. Kinetic study of template removal of MCM-41 nanostructured material. *Journal of Thermal Analysis and Calorimetry*. 2004; 75(2):693-698. http://dx.doi.org/10.1023/B:JTAN.0000027164.04415.7a.
16. Aquino FM, Melo DMA, Santiago RC, Melo MAF, Martinelli AE, Freitas JCO, et al. Thermal decomposition kinetics of PrMO3 (M=Ni or Co) ceramic materials via thermogravimetry. *Journal of Thermal Analysis and Calorimetry*. 2011; 104(2):701-705. http://dx.doi.org/10.1007/s10973-010-1191-0.
17. Braga RM, Barros JMF, Melo DMA, Melo MAF, Aquino FM, Freitas JCO, et al. Kinetic study of template removal of MCM-41 derived from rice husk ash. *Journal of Thermal Analysis and Calorimetry*. 2013; 111(2):1013-1018. http://dx.doi.org/10.1007/s10973-012-2516-y.
18. Fontes MSB, Melo DMA, Barros JMF, Braga RM, Melo MAF and Fontes VA. Kinetic study of CTMA+ removal from the pores of the Ti-MCM-41 molecular sieve. *Journal of Thermal Analysis and Calorimetry*. 2015; 119(1):197-204. http://dx.doi.org/10.1007/s10973-014-4099-2.
19. Beck JS, Vartuli JC, Roth WJ, Leonowicz ME, Kresge CT, Schmitt KD, et al. A new family of mesoporous molecular sieves prepared with liquid crystal templates. *Journal of the American Chemical Society*. 1992; 114(27):10834-10843. http://dx.doi.org/10.1021/ja00053a020.
20. Costa MJF. *Síntese e caracterização de materiais nanoporosos para pirólise catalítica de óleos pesados*. [Dissertation]. Natal: Universidade Federal do Rio Grande do Norte; 2008.
21. Gomes EL. *Síntese de peneiras moleculares contendo nióbio ou titânio e aplicação em epoxidação catalítica*. [Thesis]. São Carlos: Universidade Federal de São Carlos; 2005.
22. Blasco T, Camblor MA, Corma A and Perez-Pariente J. The state of Ti in titanoalumino silicates isomorphous with zeolite beta. *Journal of the American Chemical Society*. 1993; 115(25):11806-11813. http://dx.doi.org/10.1021/ja00078a020.
23. Eimer GA, Chanquia CM, Sapag K and Herrero ER. The role of different parameters of synthesis in the final structure of Ti-containing mesoporous materials. *Microporous and Mesoporous Materials*. 2008; 116(1-3):670-676. http://dx.doi.org/10.1016/j.micromeso.2008.05.040.
24. Ng Y-C, Jei C-Y and Shamsuddin M. Titanosilicate ETS-10 derived from rice husk ash. *Microporous and Mesoporous Materials*. 2009; 122(1-3):195-200. http://dx.doi.org/10.1016/j.micromeso.2009.03.001.